

Superdirective Arrays with Finite-Length Dipoles: Modeling and New Perspectives

Konstantinos Dovelos, Stylianos D. Assimonis, Hien Quoc Ngo, and Michail Matthaiou
Centre for Wireless Innovation, Queen’s University Belfast, Belfast, U.K.
Email: {k.dovelos, s.assimonis, hien.ngo, m.matthaiou}@qub.ac.uk

Abstract—Dense arrays can facilitate the integration of multiple antennas into finite volumes. In addition to the compact size, sub-wavelength spacing enables superdirectivity for endfire operation, a phenomenon that has been mainly studied for isotropic and infinitesimal radiators. In this work, we focus on linear dipoles of arbitrary yet finite length. Specifically, we first introduce an array model that accounts for the sinusoidal current distribution (SCD) on very thin dipoles. Based on the SCD, the loss resistance of each dipole antenna is precisely determined. Capitalizing on the derived model, we next investigate the maximum achievable rate under a fixed power constraint. The optimal design entails conjugate power matching along with maximizing the array gain. Our theoretical analysis is corroborated by the method of moments under the thin-wire approximation, as well as by full-wave simulations. Numerical results showcase that a super-gain is attainable with high radiation efficiency when the dipole antennas are not too short and thin.

I. INTRODUCTION

Multiple-input multiple-output (MIMO) systems have shaped modern wireless communications thanks to their unique capabilities, ranging from spatial multiplexing to sharp beamforming [1]. However, deploying a massive antenna array entails several challenges, such as high power consumption and size. To this end, compact arrays with sub-wavelength spacing emerge as a promising solution for beyond massive MIMO communication [2]. In addition to the small footprint of dense arrays, extremely large power gains can be attained by exploiting the mutual coupling of closely spaced antennas, a concept known as *superdirectivity*. Specifically, Uzkov [3] theoretically showed that for a uniform linear array (ULA) with N isotropic elements and a vanishingly small interelement spacing, the maximum array directivity approaches N^2 . This astonishing theoretical result has ignited a great research interest in the fundamental limits of phased arrays since then.

On the negative side, it is known that superdirectivity requires high antenna currents, which can undermine its implementation in practice [4]. This problem is exacerbated when employing a large number of antenna elements. A stream of prominent papers (e.g., [5]–[11], and references therein) investigated the performance of dense antenna arrays, yet considering rather simplistic antenna models. In particular, they assumed either isotropic radiators or Hertzian dipoles. However, the latter have infinitely large input reactance; thus, impedance matching is impossible as highlighted also in [11]. Moreover, electrically small antennas suffer from poor radiation efficiency in general. From the related literature, we distinguish [12] which studied near-field MIMO

communication with half-wavelength dipoles. Yet, existing works on superdirectivity overlook the physical dimensions of the array elements, which can have great impact on the radiation efficiency of the system. In this paper, we aim to fill this gap in the literature and shed light on the fundamentals of superdirectivity with linear dipoles. The contributions of the paper are summarized as follows:

- We provide an electromagnetic model for arrays of dipoles with arbitrary length. To facilitate analysis, a sinusoidal current distribution (SCD) [13] is assumed on each dipole. Leveraging the SCD, the loss resistance of each dipole antenna is analytically determined. Note that ohmic losses play a key role in the performance of superdirectivity [13, Ch. 6], and hence their proper modeling is of the utmost importance.
- Building upon the derived array model, we study the achievable rate under a fixed power constraint. In particular, the optimal design entails single-port power matching based on the notion of active impedance, which eliminates reflection losses; thus, it guarantees maximal power transfer between the voltage sources and the antenna elements in the presence of mutual coupling. Furthermore, beamforming is performed by maximizing the array gain. In this way, a super-gain is attained whilst increasing the energy efficiency of the system.
- Since the SCD assumption is accurate for infinitely thin wires, we validate our theoretical findings by the method of moments (MoM) and full-wave simulations with 4NEC2 [14]. For the MoM, a comprehensive framework relying on the antenna currents obtained by Hallén’s integral equations (IEs) is presented. It is then shown that the SCD-based model produces accurate results for coupled dipoles of finite radius. Consequently, the proposed model can be used to theoretically study superdirectivity without resorting to cumbersome full-wave simulations.
- Our analysis reveals the interplay between dipoles’ dimensions and superdirectivity. Particularly, it is demonstrated that increasing the dipoles’ length to specific values yields higher array gain with smaller antenna currents than short antennas. This novel observation can facilitate the efficient implementation of superdirective arrays for beyond 5G applications, ranging from wireless power transfer to nonterrestrial communications.

Notation: \mathbf{a} is a vector; \mathbf{A} is a matrix; $[\mathbf{A}]_{i,j}$ is the (i, j) th entry of \mathbf{A} ; $(\cdot)^T$, $(\cdot)^*$, and $(\cdot)^H$ denote the transpose, conjugate, and

conjugate transpose, respectively; $\|\mathbf{a}\|$ is the l_2 -norm of \mathbf{a} ; $\mathbf{a} \cdot \mathbf{b}$ is the inner product between \mathbf{a} and \mathbf{b} ; \mathbf{I}_N is the $N \times N$ identity matrix; and $\text{Re}\{\cdot\}$ is the real part of a complex variable.

II. MODEL OF DIPOLE ARRAY

In this section, we propose an array model for lossy antennas based on electromagnetic theory. Consider an array of N linear dipoles, each having length ℓ and radius ρ . All dipoles are parallel to the z -axis and are center-fed by voltage sources which induce antenna currents. We next assume that the current distribution on each dipole n has approximately the form [13, Ch. 4]

$$I_n(z') \approx I_n(0) \frac{\sin\left(\frac{k\ell}{2} - k|z'|\right)}{\sin\left(\frac{k\ell}{2}\right)}, \quad |z'| \leq \ell/2, \quad (1)$$

where $I_n(0) \in \mathbb{C}$ is the input current, $k = 2\pi/\lambda$ is the wavenumber, and λ is the carrier wavelength.

A. Radiated Power

Let $(r \cos \phi \sin \theta, r \sin \phi \sin \theta, r \cos \theta)$ be the receiver (Rx) location, where $r, \phi \in [0, 2\pi]$, and $\theta \in [0, \pi]$ are the radial distance, azimuth angle, and polar angle, respectively. The Rx is in the far-field zone of the antenna array. The magnitude of the electric field at the Rx is then specified as [13, Ch. 4]

$$E_\theta = \frac{jZ_0 e^{-jk r} \cos\left(\frac{k\ell}{2} \cos \theta\right) - \cos\left(\frac{k\ell}{2}\right)}{2\pi r \sin\left(\frac{k\ell}{2}\right) \sin \theta} \sum_{n=0}^{N-1} e^{jk \hat{\mathbf{r}} \cdot \mathbf{r}_n} I_n(0), \quad (2)$$

where Z_0 denotes the characteristic impedance of free-space, $\hat{\mathbf{r}} = (\cos \phi \sin \theta, \sin \phi \sin \theta, \cos \theta)^T$ is the unit radial vector along the Rx direction, and $\mathbf{r}_n \in \mathbb{R}^{3 \times 1}$ is the position vector of the n th antenna. The radiation intensity [W/sr] is written in vector form as

$$U \triangleq \frac{|E_\theta|^2}{2Z_0} r^2 = \frac{Z_0}{8\pi^2} F^2(\theta) |\mathbf{a}^H(\theta, \phi) \mathbf{i}|^2, \quad (3)$$

where $F(\theta) = [\cos(k\ell/2 \cos \theta) - \cos(k\ell/2)] / [\sin(k\ell/2) \sin \theta]$ corresponds to the field pattern of an individual dipole, $\mathbf{i} = [I_0(0), \dots, I_{N-1}(0)]^T \in \mathbb{C}^{N \times 1}$ is the vector of input currents, and $\mathbf{a}(\theta, \phi) = [e^{-jk \hat{\mathbf{r}} \cdot \mathbf{r}_0}, \dots, e^{-jk \hat{\mathbf{r}} \cdot \mathbf{r}_{N-1}}]^T \in \mathbb{C}^{N \times 1}$ is the array response vector. Using (3), the power radiated by the antenna array is

$$P_{\text{rad}} = \int_0^\pi \int_0^{2\pi} U \sin \theta d\theta d\phi = \frac{1}{2} \mathbf{i}^H \mathbf{Z}_{\text{real}} \mathbf{i}, \quad (4)$$

where $\mathbf{Z}_{\text{real}} \in \mathbb{R}^{N \times N}$ is the real-valued matrix with entries

$$[\mathbf{Z}_{\text{real}}]_{n,m} = \frac{Z_0}{4\pi^2} \int_0^\pi \int_0^{2\pi} e^{-jk \hat{\mathbf{r}} \cdot (\mathbf{r}_n - \mathbf{r}_m)} F^2(\theta) \sin \theta d\theta d\phi. \quad (5)$$

Remark 1. Expression (2) relies on the pattern multiplication principle, whereby the electric field is the product of the array factor $\mathbf{a}^H \mathbf{i}$ and the field pattern $F(\theta)$ of an isolated dipole radiating in free-space. This implies that the current distribution on each dipole is not affected by the presence of other antennas, and hence can be considered as sinusoidal. The accuracy of this postulate is further examined in Section IV-C.

B. Input Power and Array Gain

Realistic antennas exhibit a loss resistance which leads to heat dissipation. Because of the *skin effect* of conductive wires carrying an alternating current, the loss resistance per unit length is given by [13, Eq. (2-90b)]

$$\bar{R}_{\text{loss}} = \frac{1}{2\rho} \sqrt{\frac{f\mu}{\pi\sigma}}, \quad (6)$$

where f is the carrier frequency, μ is the permeability of free-space, and σ is the conductivity of the wire material. Under the SCD in (1), the loss resistance relative to the input current $I_n(0)$ is given by

$$R_{\text{loss}} = \bar{R}_{\text{loss}} \int_{-\ell/2}^{\ell/2} \left| \frac{I_n(z')}{I_n(0)} \right|^2 dz' = \frac{k\ell - \sin(k\ell)}{4k\rho \sin^2\left(\frac{k\ell}{2}\right)} \sqrt{\frac{f\mu}{\pi\sigma}}, \quad (7)$$

which yields the overall power loss

$$P_{\text{loss}} = \frac{1}{2} \sum_{n=0}^{N-1} R_{\text{loss}} |I_n(0)|^2 = \frac{1}{2} R_{\text{loss}} \|\mathbf{i}\|^2. \quad (8)$$

As a result, the input power at the antenna ports is

$$P_{\text{in}} = P_{\text{loss}} + P_{\text{rad}} = \frac{1}{2} \mathbf{i}^H (R_{\text{loss}} \mathbf{I}_N + \mathbf{Z}_{\text{real}}) \mathbf{i} = \frac{1}{2} \mathbf{i}^H \text{Re}\{\mathbf{Z}_{\text{in}}\} \mathbf{i}, \quad (9)$$

where $\mathbf{Z}_{\text{in}} \triangleq R_{\text{loss}} \mathbf{I}_N + \mathbf{Z}$ is the input impedance matrix of the array; $\mathbf{Z} \in \mathbb{C}^{N \times N}$, with $\text{Re}\{\mathbf{Z}\} = \mathbf{Z}_{\text{real}}$, is the input impedance matrix for lossless antennas. Finally, the array gain is defined as

$$G(\theta, \phi) \triangleq \frac{4\pi U}{P_{\text{in}}} = \frac{Z_0 F^2(\theta)}{\pi} \frac{|\mathbf{a}^H(\theta, \phi) \mathbf{i}|^2}{\mathbf{i}^H \text{Re}\{\mathbf{Z}_{\text{in}}\} \mathbf{i}}, \quad (10)$$

and the power at the Rx is determined as

$$P_r = P_{\text{in}} \left(\frac{\lambda}{4\pi r} \right)^2 G(\theta, \phi), \quad (11)$$

where an isotropic receiving antenna has been assumed.

C. Total Power and Matching Efficiency

In a practical scenario, the dipoles are driven by voltage sources. To this end, we consider that a voltage source is connected to each antenna port n through the impedance $Z_{M,n}$ used for single-port power matching.¹ The total power consumption of the array is now determined as

$$P_{\text{total}} = \frac{1}{2} \mathbf{i}^H \text{Re}\{\mathbf{Z}_M\} \mathbf{i} + P_{\text{in}} = \frac{1}{2} \mathbf{i}^H (\text{Re}\{\mathbf{Z}_M\} + \text{Re}\{\mathbf{Z}_{\text{in}}\}) \mathbf{i}, \quad (12)$$

where $\mathbf{Z}_M = \text{diag}(Z_{M,0}, \dots, Z_{M,N-1})$. For a given P_{total} , the received power is finally recast as

$$P_r = \eta P_{\text{total}} \left(\frac{\lambda}{4\pi r} \right)^2 G(\theta, \phi), \quad (13)$$

¹Multi-port matching requires inter-connections across all antenna ports. Thus, it can become very complicated in massive antenna arrays [15], [16].

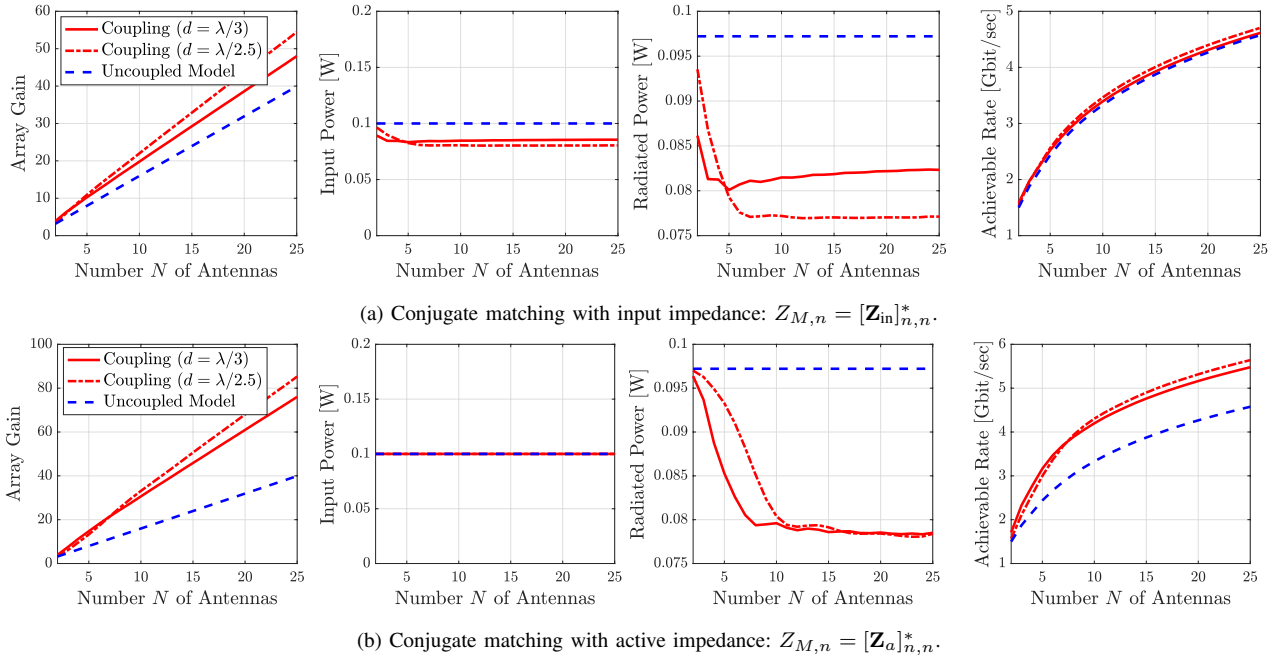


Fig. 1: Results versus number of antennas for endfire ULA with interelement spacing d . The elements have $\ell = \lambda/2$ and $\rho = \lambda/2000$, are made of copper with conductivity $\sigma = 5.7 \times 10^7$ S/m, and are placed along the x -axis, i.e., $\mathbf{r}_n = (nd, 0, 0)$. The Rx is at $r = 500$ m and $(\theta, \phi) = (\pi/2, 0)$. The other parameters are: $f = 10$ GHz, $W = 1$ GHz, $P_t = 200$ mW, and $\sigma_n^2 = -174$ dBm/Hz.

where $\eta \triangleq P_{in}/P_{total} \in [0, 1/2]$ is the matching efficiency accounting for potential reflection losses due to impedance mismatch. With perfect matching, $\eta = 1/2$, which implies that half of the total power is delivered to the antenna array [17].

III. OPTIMAL DESIGN UNDER MUTUAL COUPLING

A. Beamforming

The achievable rate [bit/sec] is specified as

$$\begin{aligned} R &= W \log_2 \left(1 + \frac{P_r}{W\sigma_n^2} \right) \\ &= W \log_2 \left(1 + \frac{P_{total}}{W\sigma_n^2} \frac{\lambda^2}{(4\pi r)^2} \eta G(\theta, \phi) \right), \end{aligned} \quad (14)$$

where W is the signal bandwidth, and σ_n^2 is the noise power density at the Rx. We next seek to find \mathbf{i} that maximizes R under the constraint $P_{total} \leq P_t$, where P_t denotes the maximum power budget of the system. By properly scaling the vector \mathbf{i} of currents, $P_{total} = P_t$ and $\eta G(\theta, \phi)$ remains unchanged. Then, the initial problem of maximizing R becomes equivalent to the unconstrained problem

$$\max_{\mathbf{i}} \eta G(\theta, \phi) = \frac{\mathbf{i}^H \mathbf{a}(\theta, \phi) \mathbf{a}^H(\theta, \phi) \mathbf{i}}{\mathbf{i}^H (\text{Re}\{\mathbf{Z}_M\} + \text{Re}\{\mathbf{Z}_{in}\}) \mathbf{i}}. \quad (15)$$

The objective in (15) is a generalized Rayleigh quotient, and hence it admits the solution $\mathbf{i} = \mathbf{C}^{-1} \mathbf{a}(\theta, \phi)$, where $\mathbf{C} \triangleq \text{Re}\{\mathbf{Z}_M\} + \text{Re}\{\mathbf{Z}_{in}\}$ for notational convenience. Given the above, the optimal current vector is

$$\mathbf{i} = \sqrt{\frac{2P_t}{\mathbf{a}^H(\theta, \phi) \mathbf{C}^{-1} \mathbf{a}(\theta, \phi)}} \mathbf{C}^{-1} \mathbf{a}(\theta, \phi). \quad (16)$$

B. Single-Port Matching

Mutual coupling alters the input impedance of each dipole. Thus, typical conjugate matching, i.e., $Z_{M,n} = [\mathbf{Z}_{in}]_{n,n}^*$, will result in significant reflection losses. To avoid this, we leverage the notion of *active impedance*, which follows from the relationship $\mathbf{v} = \mathbf{Z}_{in} \mathbf{i} = \mathbf{Z}_a \mathbf{i}$, where $\mathbf{v} \in \mathbb{C}^{N \times 1}$ is the vector of voltages at the antenna ports. The active impedance matrix $\mathbf{Z}_a \in \mathbb{C}^{N \times N}$ is diagonal with entries

$$[\mathbf{Z}_a]_{n,n} = \left(R_{\text{loss}} + [\mathbf{Z}]_{n,n} + \sum_{m=0, m \neq n}^{N-1} [\mathbf{Z}]_{n,m} \frac{i_m}{i_n} \right). \quad (17)$$

The reflection coefficient for the n th port is defined as [18]

$$\Gamma_n \triangleq \frac{[\mathbf{Z}_a]_{n,n} - Z_{M,n}^*}{[\mathbf{Z}_a]_{n,n} + Z_{M,n}}. \quad (18)$$

From (18), it is evident that optimal matching is accomplished for $Z_{M,n} = [\mathbf{Z}_a]_{n,n}^*$. Note that the active impedance matrix hinges on the vector \mathbf{i} of currents, and hence it changes with (θ, ϕ) . Consequently, reflectionless operation is possible only for a specific scanning direction (θ, ϕ) . The entries of the impedance matrix \mathbf{Z} used in (17) are calculated by the induced EMF method [19, Ch. 25]. Under the optimal matching strategy, the total power becomes

$$\begin{aligned} P_{total} &= \frac{1}{2} \text{Re} \{ \mathbf{i}^H (\mathbf{Z}_a^* + \mathbf{Z}_{in}) \mathbf{i} \} \\ &= \mathbf{i}^H \text{Re}\{\mathbf{Z}_{in}\} \mathbf{i}, \end{aligned} \quad (19)$$

which is exactly twice the input power. For this reason, the beamforming problem (15) reduces to maximizing the array

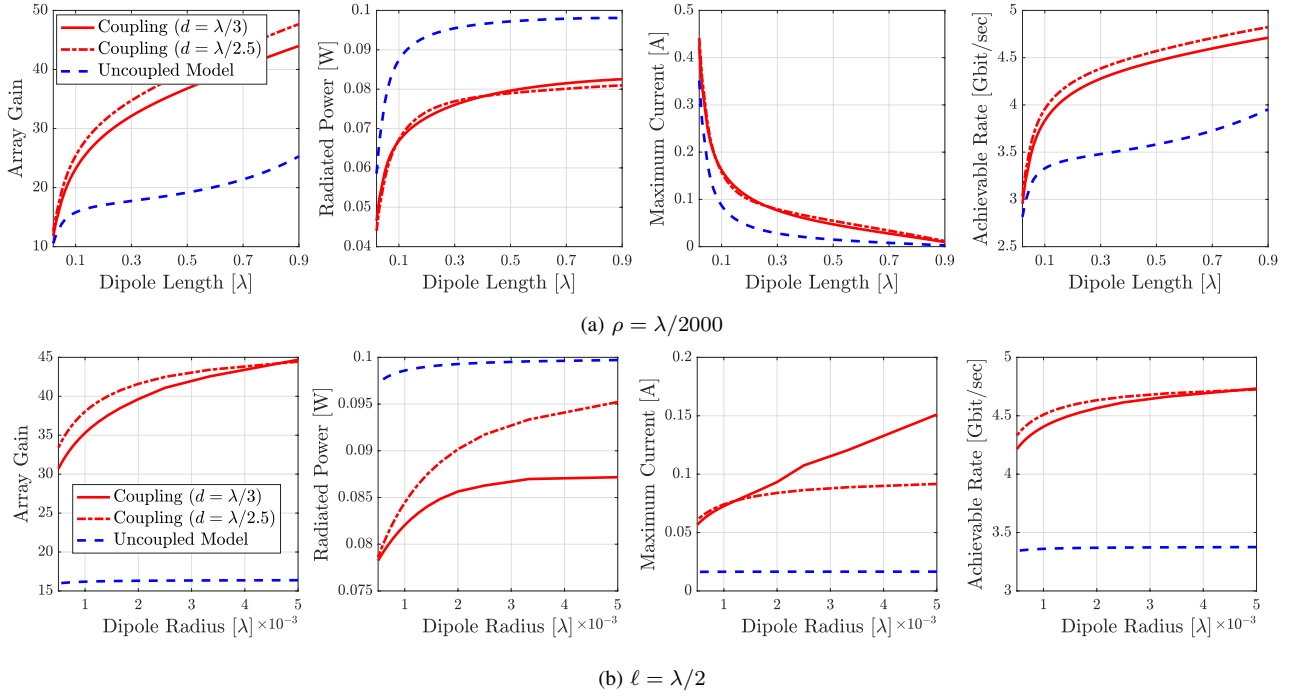


Fig. 2: Results for endfire ULA with $N = 10$ elements and interelement spacing d . The elements are made of copper with conductivity $\sigma = 5.7 \times 10^7$ S/m, and are placed along the x -axis, i.e., $\mathbf{r}_n = (nd, 0, 0)$. The Rx is at $r = 500$ m and $(\theta, \phi) = (\pi/2, 0)$. The other parameters are: $f = 10$ GHz, $W = 1$ GHz, $P_t = 200$ mW, and $\sigma_n^2 = -174$ dBm/Hz.

gain, i.e., $\max_i G(\theta, \phi)/2 = \max_i G(\theta, \phi)$. Given that, the maximum array gain at the Rx direction (θ, ϕ) is

$$G_{\max}(\theta, \phi) = \frac{Z_0 F^2(\theta)}{\pi} \mathbf{a}^H(\theta, \phi) \text{Re}\{\mathbf{Z}_{\text{in}}\}^{-1} \mathbf{a}(\theta, \phi). \quad (20)$$

C. Uncoupled Model

In the absence of mutual coupling, $\mathbf{Z}_{\text{real}} = R_i \mathbf{I}_N$, where $R_i \triangleq [\mathbf{Z}_{\text{real}}]_{n,n}$ defines the input resistance of a lossless dipole, i.e., radiation resistance divided by $\sin^2(k\ell/2)$ [13, Ch. 8]. Then, $P_{\text{rad}} = \frac{1}{2} R_i \|\mathbf{i}\|^2$, which is exactly the power emitted by N uncoupled antennas. Moreover, (16) reduces to

$$\mathbf{i} = \sqrt{\frac{P_t}{N(R_{\text{loss}} + R_i)}} \mathbf{a}(\theta, \phi). \quad (21)$$

Under (21), $G_{\max}(\theta) = \frac{Z_0}{\pi(R_{\text{loss}} + R_i)} F^2(\theta) N = O(N)$, which is the conventional power gain that increases linearly with the number N of antennas.

IV. NUMERICAL RESULTS AND DISCUSSION

A. Performance versus Number of Antennas

In this numerical experiment, we consider half-wavelength dipoles. From Fig. 1, we first observe the superdirectivity effect thanks to strong mutual coupling. The importance of suitable impedance matching is also showcased in Fig. 1(a), where reflection losses cancel out the benefit of superdirectivity. It is worth stressing that the array gain is reduced when $Z_{M,n} = [\mathbf{Z}_{\text{in}}]_{n,n}^*$ because the optimal excitation (16) maximizes the product $\eta G(\theta, \phi)$.

Under perfect matching, the reduction in the radiated power due to heat dissipation is compensated by the large increase in the directivity. As a result, the achievable rate is significantly enhanced by employing a sub-wavelength spacing, whilst meeting the power constraint $P_{\text{total}} \leq 200$ mW. In short, superdirectivity does not necessarily compromise the energy efficiency of the system. Regarding the uncoupled case, the radiated power and ohmic losses remain constant versus N as

$$P_{\text{rad}} = \frac{1}{2} \frac{R_i}{R_{\text{loss}} + R_i} P_t, \quad (22)$$

$$P_{\text{loss}} = \frac{1}{2} \frac{R_{\text{loss}}}{R_{\text{loss}} + R_i} P_t. \quad (23)$$

This comes in sharp contrast to the superdirective case, where ohmic losses become dominant for a large number of antennas. To mitigate this problem, one can adopt longer dipoles to boost the transmission efficiency of each array element.

B. Effect of Dipole Dimensions

From antenna theory, we know that longer dipoles have higher element directivity and radiation resistance [20]. Hence, they can be beneficial in terms of transmission characteristics. Furthermore, the elements of \mathbf{Z}_{in} become larger for $\ell > \lambda/2$, which results in smaller antenna current values as $\mathbf{i} \propto \mathbf{Z}_{\text{in}}^{-1} \mathbf{a}$. This behavior becomes more evident in the uncoupled case, where $\mathbf{i} \propto (R_{\text{loss}} + R_i)^{-1/2}$. This finding is validated in Fig. 2(a) for $0.02\lambda \leq \ell \leq 0.9\lambda$. In short, increasing the dipole length up to 0.9λ improves the radiation efficiency of superdirectivity. Regarding dipoles' radius, (7) shows that the

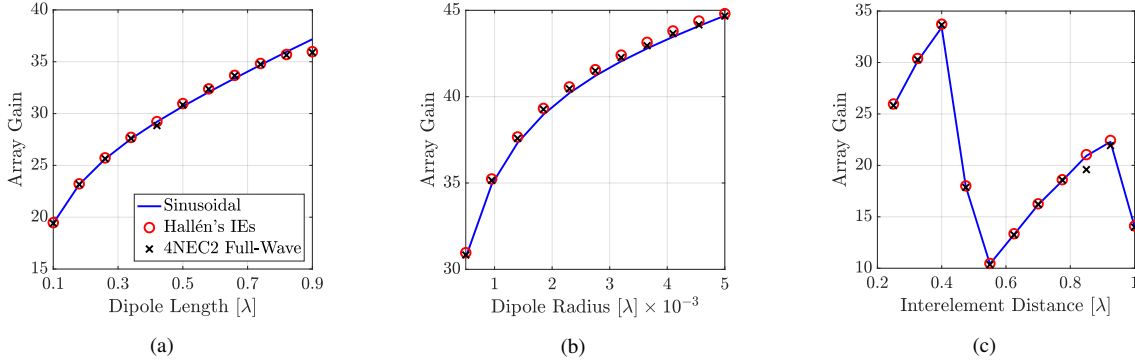


Fig. 3: $G_{\max}(\pi/2, 0)$ for an endfire ULA with $N = 10$ elements. The antennas are made of copper with conductivity $\sigma = 5.7 \times 10^7$ S/m, and are placed along the x -axis. In the MoM-based approach and full-wave simulation, $2M + 1 = 401$ samples have been used. In (a), (b), and (c), $\rho = \lambda/2000$, $\ell = \lambda/2$, and $d = \lambda/3$, while the respective parameter varies accordingly.

loss resistance is inversely proportional to ρ . Consequently, increasing the dipoles' radius will decrease the ohmic losses of the array. Figure 2(b) demonstrates the benefit of employing thicker dipoles for $\lambda/2000 \leq \rho \leq \lambda/200$.

C. Array Model Validation

It is known that the SCD is very accurate for dipoles of vanishing radius, i.e., $\rho \rightarrow 0$ [13]. It is therefore important to validate our results for thin dipoles of finite radius, which are closely spaced. For this purpose, we now recall that, under the *thin-wire approximation*, E_θ takes the form [19, Ch. 25]

$$E_\theta = jZ_0k \frac{e^{-jkr}}{4\pi r} \sin\theta \sum_{n=0}^{N-1} e^{jk\hat{\mathbf{r}} \cdot \mathbf{r}_n} S_n(\theta), \quad (24)$$

where

$$S_n(\theta) \triangleq \int_{-\ell/2}^{\ell/2} I_n(z') e^{jkz' \cos\theta} dz' \quad (25)$$

is the space factor of the n th dipole, i.e., line source of length ℓ . The current distribution $I_n(z')$ on the n th antenna is the result of the driving voltages and their mutual interaction. Thus, the current distributions satisfy a system of coupled Hallén's IEs, which effectively capture the electromagnetic coupling between adjacent antennas.² These IEs are numerically solved by the MoM to obtain $\{I_n(z')\}_{n=0}^{N-1}$ for *given input voltages*. To this end, the basis expansion

$$I_n(z') = \sum_{m=-M}^M I_n(m\Delta) B(z' - m\Delta) \quad (26)$$

is employed, where $B(\cdot)$ is a basis function, $2M + 1$ is the total number of samples, whereas $\Delta = \ell/(2M)$ is the sample spacing. Considering the pulse basis function

$$B(z' - m\Delta) = \begin{cases} 1, & |z' - m\Delta| \leq \frac{\Delta}{2}, \\ 0, & \text{otherwise} \end{cases}, \quad (27)$$

the space factor is recast as [19, Ch. 25]

$$S_n(\theta) = \sum_{m=-M}^M I_n(m\Delta) e^{jkm\Delta \cos\theta} \frac{\sin(k/2 \cos\theta \Delta)}{k/2 \cos\theta}. \quad (28)$$

²Note that Hallén's IEs hold for delta-gap input voltages.

Based on (24) and (28), the electric field of the N coupled dipoles can be precisely characterized. Next, the radiation intensity becomes

$$U = \frac{Z_0 k^2}{32\pi^2} \left| \sum_{n=0}^{N-1} e^{jk\hat{\mathbf{r}} \cdot \mathbf{r}_n} S_n(\theta) \right|^2, \quad (29)$$

whilst the radiated power is conveniently computed as

$$P_{\text{rad}} = \frac{1}{2} \text{Re} \{ \mathbf{v}_{\text{in}}^H \mathbf{i}_{\text{in}} \}, \quad (30)$$

where $\mathbf{i}_{\text{in}} \triangleq [I_0(0), \dots, I_{N-1}(0)]^T \in \mathbb{C}^{N \times 1}$ and $\mathbf{v}_{\text{in}} \in \mathbb{C}^{N \times 1}$ are the vectors of input currents and voltages, respectively. Lastly, the power loss due to heat dissipation at the n th dipole is

$$P_{\text{loss},n} \triangleq \frac{1}{2} \bar{R}_{\text{loss}} \int_{-\ell/2}^{\ell/2} |I_n(z')|^2 dz' = \frac{1}{2} \bar{R}_{\text{loss}} \sum_{m=-M}^M |I_n(m\Delta)|^2 \Delta, \quad (31)$$

which results in the overall power loss

$$P_{\text{loss}} = \sum_{n=0}^{N-1} P_{\text{loss},n}. \quad (32)$$

The following algorithm describes the steps to evaluate the array gain using the electric field IEs for coupled dipoles.

Algorithm Array Gain based on the MoM

- 1: Assume sinusoidal distribution and calculate the antenna current vector \mathbf{i} using (16).
 - 2: Specify the input voltages as $\mathbf{v}_{\text{in}} = \mathbf{Z}\mathbf{i}$, where \mathbf{Z} is computed by the induced EMF method for lossless antennas and SCD.
 - 3: For given \mathbf{v}_{in} , obtain $\{I_n(z')\}_{n=0}^{N-1}$ from Hallén's IEs.
 - 4: Compute $G(\theta, \phi) = 4\pi U/P_{\text{in}}$ using (29), (30) and (32).
-

Remark 2. The SCD renders the impedance matrix \mathbf{Z} independent of the input voltages [19]. As a result, the entries of \mathbf{Z} hinge solely on the array geometry and antenna characteristics. This facilitates the computation of \mathbf{Z} , which is used to theoretically determine the optimal current excitation via (16).

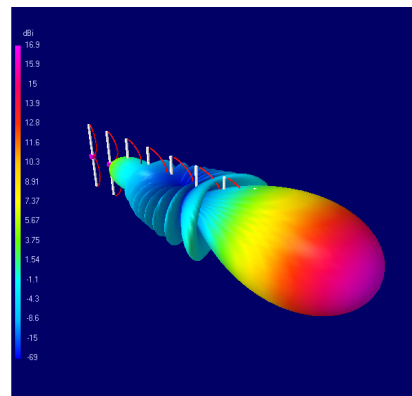
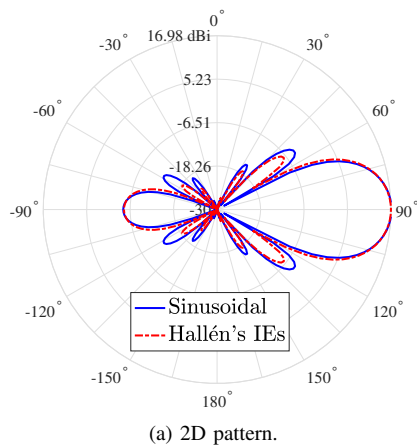


Fig. 4: $G(\theta, \phi)$ for an 10-element ULA along the x -axis at $f = 10$ GHz, $d = \lambda/2.5$, and \mathbf{i} given by (16) for $(\theta, \phi) = (\pi/2, 0)$. The dipoles are copper wires of $\ell = 0.9\lambda$ and $\rho = \lambda/200$. In the MoM approach and full-wave simulation, $2M + 1 = 401$ samples have been used.

We now examine the accuracy of the SCD assumption when calculating the array gain $G_{\max}(\pi/2, 0)$ for different dipole lengths. From Fig. 3(a), we first confirm the excellent match between the theoretical model, the MoM-based approach, and the full-wave simulation. The small discrepancy at $\ell = 0.9\lambda$ is expected, because the SCD assumption breaks down as the dipole length approaches λ [13]. From Fig. 3(b), we also see a good agreement for various dipole radii. More importantly, this holds for dipoles as thick as $\rho = \lambda/200$. Regarding the interelement spacing, the optimal one is $\lambda/2.5$ according to Fig. 3(c), which implies that the dipoles should not be placed very close to each other; similar finding were reported in [9], though for isotropic radiators. Lastly, Fig. 4 depicts the 2D and 3D gain patterns under optimal interelement separation, which were calculated using the SCD assumption, Hallén's IEs, and full-wave simulation. As expected, the maximum array gain is achieved along the endfire direction $(\pi/2, 0)$, and is 16.98 dBi (i.e., 49.88 in linear scale). In conclusion, the proposed array model can provide meaningful results, yet with much smaller computational complexity than purely numerical methods.

V. CONCLUSIONS

We studied, for the first time, the impact of dipole antenna dimensions on superdirectivity. For this purpose, we developed an array model that captures the main characteristics of linear dipoles. Capitalizing on the SCD of very thin wires, the overall ohmic losses were explicitly computed, which greatly affect the array gain. Next, the optimal beamforming problem under a fixed power constraint was addressed. As shown, a supergain can be attained without sacrificing the energy efficiency of the system when not too short and thin elements are employed. We also confirmed our findings via a MoM-based approach as well as full-wave simulations. In particular, it was demonstrated that the proposed theoretical model predicts the array gain of coupled thin dipoles with high precision.

ACKNOWLEDGEMENTS

This project has received funding from the European Research Council (ERC) under the European Union's Horizon

2020 research and innovation programme (grant agreement No. 101001331).

REFERENCES

- [1] J. Zhang *et al.*, "Prospective multiple antenna technologies for beyond 5G," *IEEE J. Sel. Areas Commun.*, vol. 38, no. 8, pp. 1637–1660, Aug. 2020.
- [2] S. Hu, F. Rusek, and O. Edfors, "Beyond massive MIMO: The potential of data transmission with large intelligent surfaces," *IEEE Trans. Signal Process.*, vol. 66, no. 10, pp. 2746–2758, May 2018.
- [3] A. Uzkov, "An approach to the problem of optimum directive antenna design," *Comptes Rendus (Doklady) de l'Academie des Sci. de l'URSS*, vol. 53, no. 1, pp. 35–38, 1946.
- [4] S. A. Schelkunoff, "A mathematical theory of linear arrays," *Bell Syst. Tech. J.*, vol. 22, no. 1, pp. 80–107, Jan. 1943.
- [5] M. L. Morris *et al.*, "Superdirectivity in MIMO systems," *IEEE Trans. Antennas Propag.*, vol. 53, no. 9, pp. 2850–2857, Sept. 2005.
- [6] N. W. Bikhazi and M. A. Jensen, "The relationship between antenna loss and superdirectivity in MIMO systems," *IEEE Trans. Wireless Commun.*, vol. 6, no. 5, pp. 1796–1802, May 2007.
- [7] T. L. Marzetta, "Super-directive antenna arrays: Fundamentals and new perspectives," in *Proc. IEEE ACSSC*, Nov. 2019.
- [8] R. J. Williams, E. de Carvalho, and T. L. Marzetta, "A communication model for large intelligent surfaces," in *Proc. IEEE ICC*, Jun. 2020.
- [9] M. T. Ivrlač and J. A. Nossek, "High-efficiency super-gain antenna arrays," in *Proc. Int. ITG WSA*, Feb. 2010, pp. 369–374.
- [10] M. T. Ivrlač and J. A. Nossek, "Toward a circuit theory of communication," *IEEE Trans. Circuits Syst.*, vol. 57, no. 7, pp. 1663–1683, Jul. 2010.
- [11] R. J. Williams *et al.*, "Multiuser MIMO with large intelligent surfaces: Communication model and transmit design," *arXiv preprint arXiv:2011.00922*, Nov. 2020.
- [12] S. Phang *et al.*, "Near-field MIMO communication links," *IEEE Trans. Circuits Syst.*, vol. 65, no. 9, pp. 3027–3036, Sep. 2018.
- [13] C. A. Balanis, *Antenna Theory: Analysis and Design*, 3rd ed., John Wiley & Sons, 2012.
- [14] W. C. Gibson, *The Method of Moments in Electromagnetics*, 2nd ed., Chapman and Hall/CRC, 2014.
- [15] T. A. de Vasconcelos *et al.*, "Matching strategies for multiantenna arrays," in *Proc. Int. ITG WSA*, Feb. 2020.
- [16] T. Laas, J. A. Nossek, and W. Xu, "Limits of transmit and receive array gain in massive MIMO," in *Proc. IEEE WCNC*, May 2020.
- [17] D. M. Pozar, *Microwave Engineering*, John Wiley & Sons, 2009.
- [18] S. D. Assimonis *et al.*, "Efficient and sensitive electrically small rectenna for ultra-low power RF energy harvesting," *Sci. Rep.*, vol. 8, Oct. 2018.
- [19] S. J. Orfanidis, *Electromagnetic Waves and Antennas*, Rutgers University, 2016.
- [20] J. D. Kraus, *Antennas*, 2nd ed., McGraw-Hill, 1988.